Bioorganic & Medicinal Chemistry Letters 30 (2020) 127400

Contents lists available at ScienceDirect

Bioorganic & Medicinal Chemistry Letters

journal homepage: www.elsevier.com/locate/bmcl

Synthesis of ^{18}F-labeled streptozotocin derivatives and an *in-vivo* kinetics study using positron emission tomography

Kenji Arimitsu[a,*], Yusuke Yagi[a], Kazuhiro Koshino[b], Yukina Nishito[a], Takahiro Higuchi[c,d], Hiroyuki Yasui[a], Hiroyuki Kimura[a,*]

[a] Department of Analytical and Bioinorganic Chemistry, Kyoto Pharmaceutical University, 5 Nakauchi-cho, Misasagi, Yamashina-ku, Kyoto 607–8414, Japan
[b] Department of Systems and Informatics, Hokkaido Information University, 59-2 Nishi-Nopporo, Ebetsu, Hokkaido 069-8585, Japan
[c] Graduate School of Medicine Dentistry and Pharmaceutical Sciences, Okayama University, 2-5-1 Shikada-cho, Kita-ku, Okayama 700-8558, Japan
[d] Department of Nuclear Medicine and Comprehensive Heart Failure Centre (CHFC), Julius-Maximilian-University of Würzburg, Oberderrbacherstr. 6, 97080 Würzburg, Germany

ARTICLE INFO

Keywords:
Streptozotocin
Glucose transporter 2
Fluorine-18 labeling
Positron emission tomography
Type-2 diabetes
Metabolic syndrome

ABSTRACT

Glucose transporter 2 (GLUT2) is involved in glucose uptake by hepatocytes, pancreatic beta cells, and absorptive cells in the intestine and proximal tubules in the kidney. Pancreatic GLUT2 also plays an important role in the mechanism of glucose-stimulated insulin secretion. In this study, novel Fluorine-18-labeled streptozotocin (STZ) derivatives were synthesized to serve as glycoside analogs for *in-vivo* GLUT2 imaging. Fluorine was introduced to hexyl groups at the 3′-positions of the compounds, and we aimed to synthesize compounds that were more stable than STZ. The nitroso derivatives exhibited relatively good stability during purification and purity analysis after radiosynthesis. We then evaluated the compounds in PET imaging and *ex-vivo* biodistribution studies. We observed high levels of radioactivity in the liver and kidney, which indicated accumulation in these organs within 5 min of administration. In contrast, the denitroso derivatives accumulated only in the kidney and bladder shortly after administration. Compounds with nitroso groups are thus expected to accumulate in GLUT2-expressing organs, and the presence of a nitroso group is essential for *in-vivo* GLUT2 imaging.

Glucose transporters (GLUTs) are membrane proteins encoded by SLC2 genes that mediate the transport of monosaccharides, polyols, and other small molecules.[1–3] Fourteen families of GLUT proteins have been identified in humans, and one or more GLUT families are expressed in every cell type. Among membrane transporters, GLUT1 is one of the most extensively studied. GLUT1 is expressed by many cells, including erythrocytes, brain cells, and cells in the blood-brain barrier. It plays an important role in glucose-metabolizing tissues.[4–7] A glucose mimic labeled with fluorine-18, 2-deoxy-2-[^{18}F]fluoro-D-glucose ([^{18}F]FDG), is the most widely used positron emission tomography (PET) probe for the detection of solid tumors and cardiovascular events due to its high affinity for GLUT1.[8] GLUT2 belongs to another family of GLUTs expressed primarily in hepatocytes, pancreatic beta cells, and absorptive cells in the intestine and kidney proximal tubules.[9] GLUT2 (K_m of ~17 mM) has a notably lower affinity for glucose than GLUT1 (K_m of 2–5 mM).[10] This unique characteristic of GLUT2 means that its rate of glucose uptake varies, even at normal and hyperglycemic plasma glucose concentrations. Previous research indicates that pancreatic GLUT2 has an important function in glucose-stimulated insulin secretion, which decreased in pancreatic beta cells with a decrease in GLUT2-expression.[11–17] Reduced levels of GLUT2 expression have been observed on the surfaces of pancreatic cells in mice fed a high-fat diet and pancreatic beta cells exposed to palmitic acid and the synthetic glucocorticoid dexamethasone.[18,19] The decrease in GLUT2 expression has been found to be the result of reduced GnT-IVa expression, which is related to the production of a complex-type glycan in the GLUT2 protein that stabilizes GLUT2 on cell surfaces by binding lectin receptors.[20,21] Decreased GnT-IVa expression is thought to be the reason why elevated free fatty acid concentrations cause nuclear exclusion and reduced expression of the transcription factors FOXA2 and HNF-1A in beta cells.[22] It has thus been suggested that GLUT2 is a very important biomolecule in the pathogenic mechanism of impaired insulin secretion and insulin resistance in type-2 diabetes. In their efforts to visualize the ribose salvage pathway, Clark et al. reported the incorporation of a ^{18}F-labeled compound into mouse hepatocytes via GLUT2.[23] They found that 2-deoxy-2-[^{18}F]fluoroarabinose was taken up by the liver through GLUT2, and that uptake by the liver was reduced in model mice with metabolic syndrome. This confirmed that GLUT2 expression by

* Corresponding authors.
E-mail addresses: arimitsu@mb.kyoto-phu.ac.jp (K. Arimitsu), hkimura@mb.kyoto-phu.ac.jp (H. Kimura).

https://doi.org/10.1016/j.bmcl.2020.127400
Received 10 April 2020; Received in revised form 3 July 2020; Accepted 6 July 2020
Available online 09 July 2020
0960-894X/

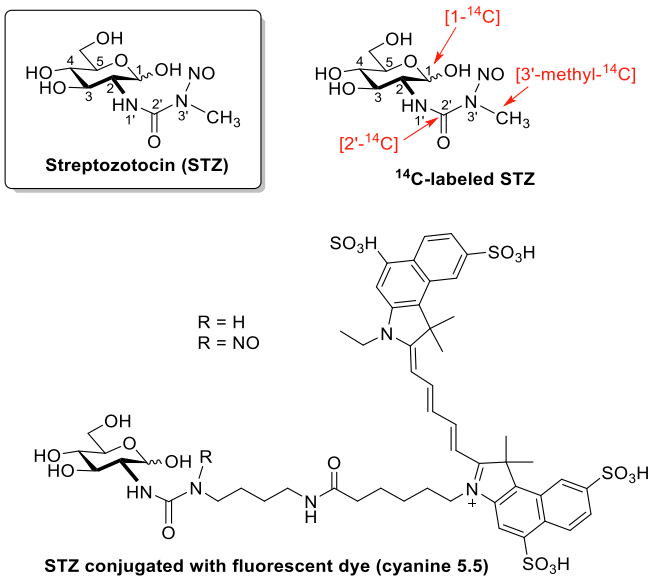

Fig. 1. Structures of STZ and known labeled STZ derivatives.

hepatocytes would decrease with the progression of type-2 diabetes. We hypothesized that the expression of GLUT2 on cell membranes would decrease as part of a negative feedback mechanism in hyperlipidemia, which would promote gluconeogenesis after lipid consumption and reduce intracellular glucose concentrations. We thus became interested in elucidating the relationship between metabolic syndrome and GLUT2 expression.

Herein we report the synthesis of ^{18}F-labeled streptozotocin (STZ) derivatives for *in-vivo* GLUT2 imaging. STZ (Fig. 1) is a D-glucosamine derivative that bears a nitrosoureido group,[24] and it is known to be taken up by cells through GLUT2.[25,26] STZ causes nitrosourea-induced cytotoxicity, and its antibacterial and antitumor activities make it biologically useful.[25,28] In fact, STZ has been approved in Japan and the United States as a drug for metastatic cancer of the pancreatic islet cells.[29] Diabetogenic activity damages beta cells in the islets of Langerhans in the pancreas. STZ has been used to establish mouse models for type-1 diabetes in the field of diabetes research.[30–32] The *in-vivo* biodistribution of STZ labeled with carbon-14 has been studied.[33,34] Carbon-14 was incorporated at the 3′-position of STZ to make it radioactive for detection, and the sugar moiety was shown to be important for the accumulation of STZ in pancreatic islets. Radioactivity also accumulated in the liver and kidney. STZ derivatives have also been conjugated to fluorescent probes[35,36] and the probes were found to be taken up selectively by insulinoma INS-1E cells used to model pancreatic beta cells. However, STZ derivatives labeled with positron-emitting nuclides have never been developed for *in-vivo* PET imaging. We synthesized novel ^{18}F-labeled STZ derivatives and evaluated their biodistribution in normal mice by performing PET imaging and an *ex-vivo* biodistribution study.

Prior to designing ^{18}F-labeled STZ, we investigated a known STZ derivative (**III**)[37] that contained a 2-fluoroethyl group as a substitute for the STZ methyl group (Scheme 1A). We synthesized the compound from 2-fluoroethylamine and D-glucosamine (Scheme 1A). We first prepared a carbamate (**I**) from 2-fluoroethylamine and disuccinimidyl carbonate and reacted it with D-glucosamine to obtain glucosaminyl urea (**II**).[38] *N*-nitrosylation of **II** with *tert*-butyl nitrite afforded derivative **III** as a white solid. However, we concluded that **III** would not be a suitable ^{18}F-labeled model compound. One reason for this was the long reaction time needed for the first step. Even if 2-[^{18}F]fluoroethylamine was used, a long reaction time did not afford **I** with a sufficient amount of radioactivity.[39] Another reason was the instability of **III** and urea **II**. We expected **III** to be unstable based on previous studies of STZ and chlorozotocin.[24,40] However, the urea precursor (**II**) also generated

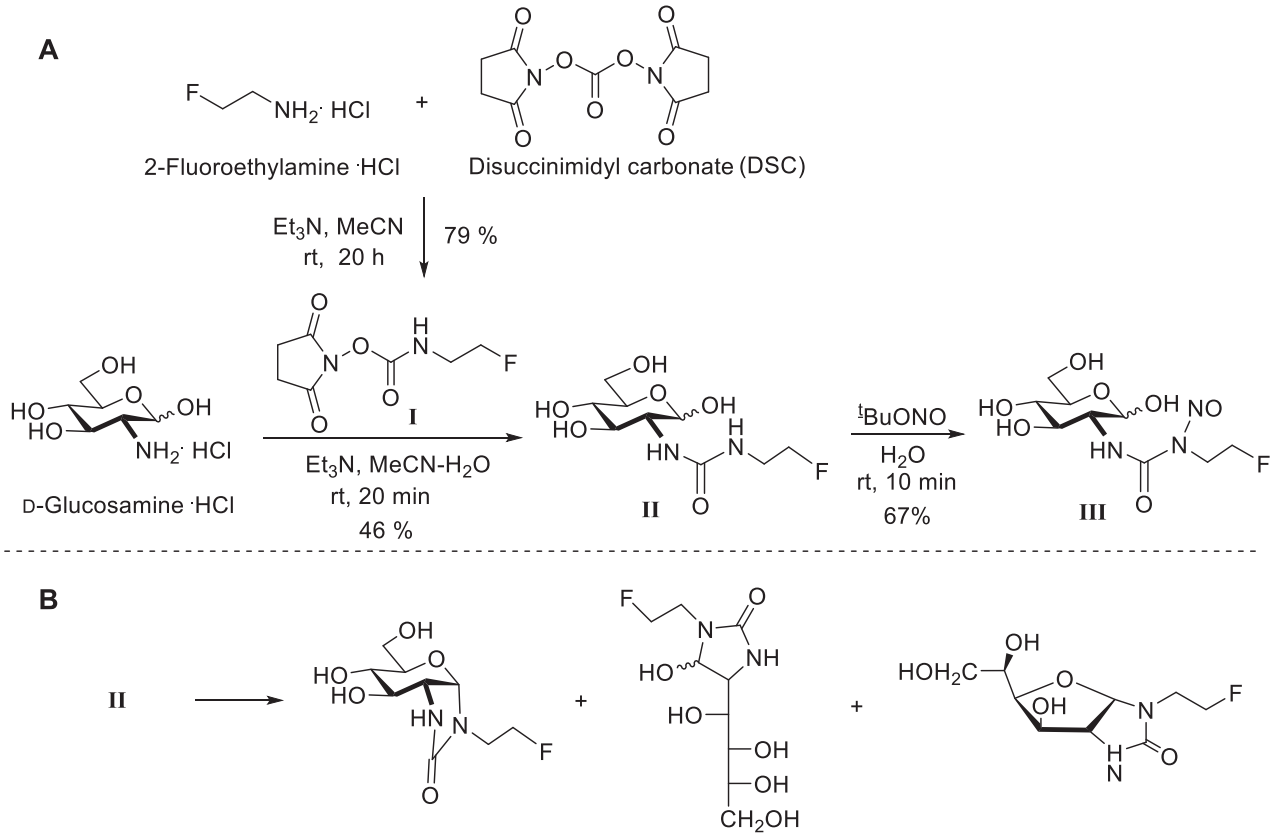

Scheme 1. Synthesis of a known fluorinated STZ derivative (**III**) and structures predicted to be obtained from the transformation of urea **II**.

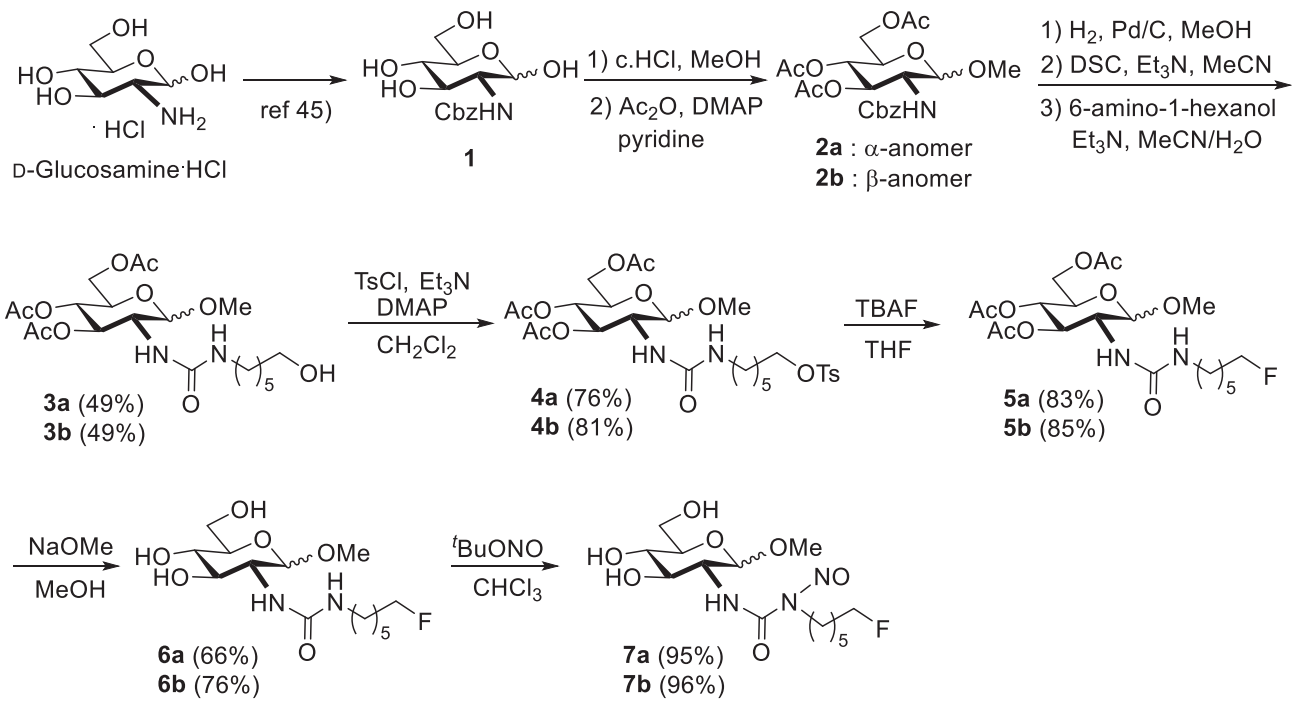

Scheme 2. Synthesis of the novel fluorinated STZ derivatives **7a** and **7b.**

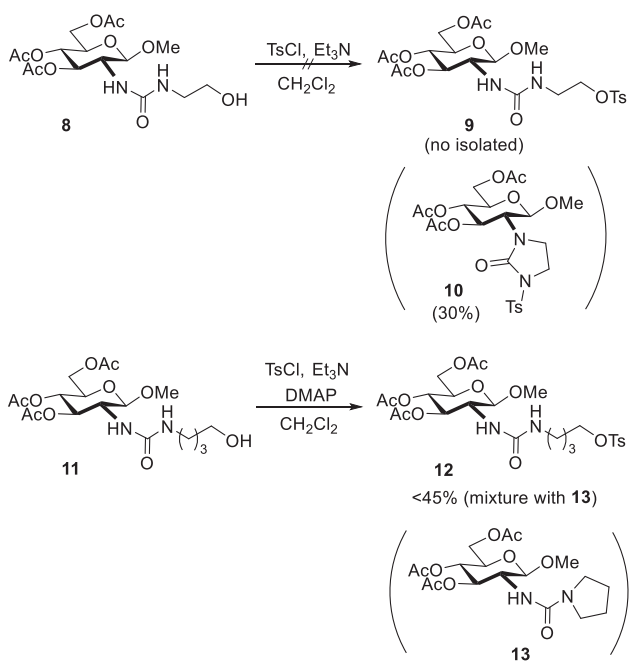

Scheme 3. Attempt of tosylation using compounds **8** and **11.**

byproducts rapidly in solution. This was attributed to cyclization of the anomeric carbon and nitrogen atoms in the urea moiety (Scheme 1B).[41] Based on these results, we decided to redesign the STZ derivatives.

Alkylating the anomeric hydroxy groups in STZ glycoside analogs has been reported to enhance their stability.[42] The compounds do not have diabetogenic activity, and their antitumor activities are similar to that of STZ.[42–44] However, it is not yet known whether glycosylation interferes with their ability to interact with GLUT2. We decided to employ this strategy to synthesize methyl glycosides. Thereby, we first obtained *N*-carbobenzyloxy-D-glucosamine (**1**)[45] from D-glucosamine hydrochloride and used it to prepare α-methyl and β-methyl glycosides **2a** and **2b** (Scheme 2). Anomeric isomers **2a** and **2b** could be separated via silica gel chromatography. The benzyloxycarbonyl protecting groups were removed, and disuccinimidyl carbonate was added for subsequent conversion to the active carbamates without purification. To perform conventional ^{18}F-fluorination of the corresponding tosylate precursor using potassium [^{18}F]fluoride, the introduction of hydroxyalkyl chain of appropriate length to the ureido moiety was investigated. Among them, the tosylation of 2-hydroxyethyl derivative **8** and 4-hydrobutyl derivative **11** prepared from **2b** to give corresponding tosylate were difficult because these compounds readily underwent intramolecular cyclization (Scheme 3). Therefore, we prepared 6-hydroxyhexylureido compounds **3a** and **3b** with 6-amino-1-hexanol in moderate yields, and subsequent tosylation of **3a** and **3b** successfully yielded **4a** and **4b** as precursors for the fluorinated compounds (Scheme

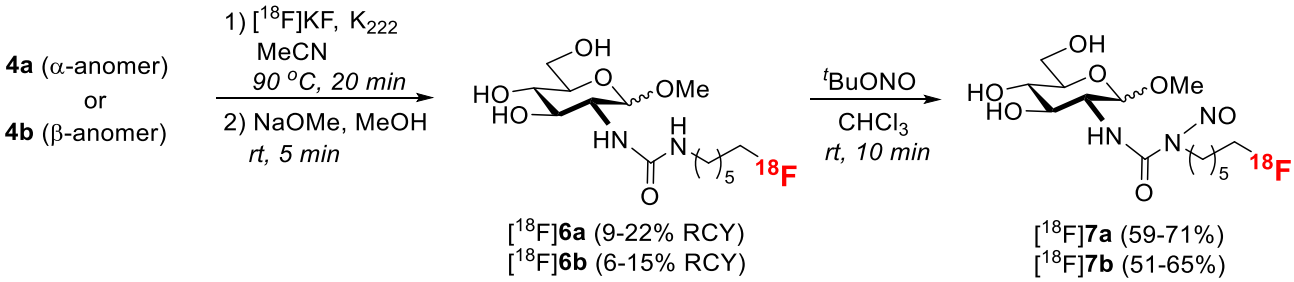

Scheme 4. Synthesis of ^{18}F-fluorinated STZ derivatives [^{18}F]**7a** and [^{18}F]**7b**. The yields shown in parentheses represent the ranges of three independent experiments (n = 3) at the end of synthesis.

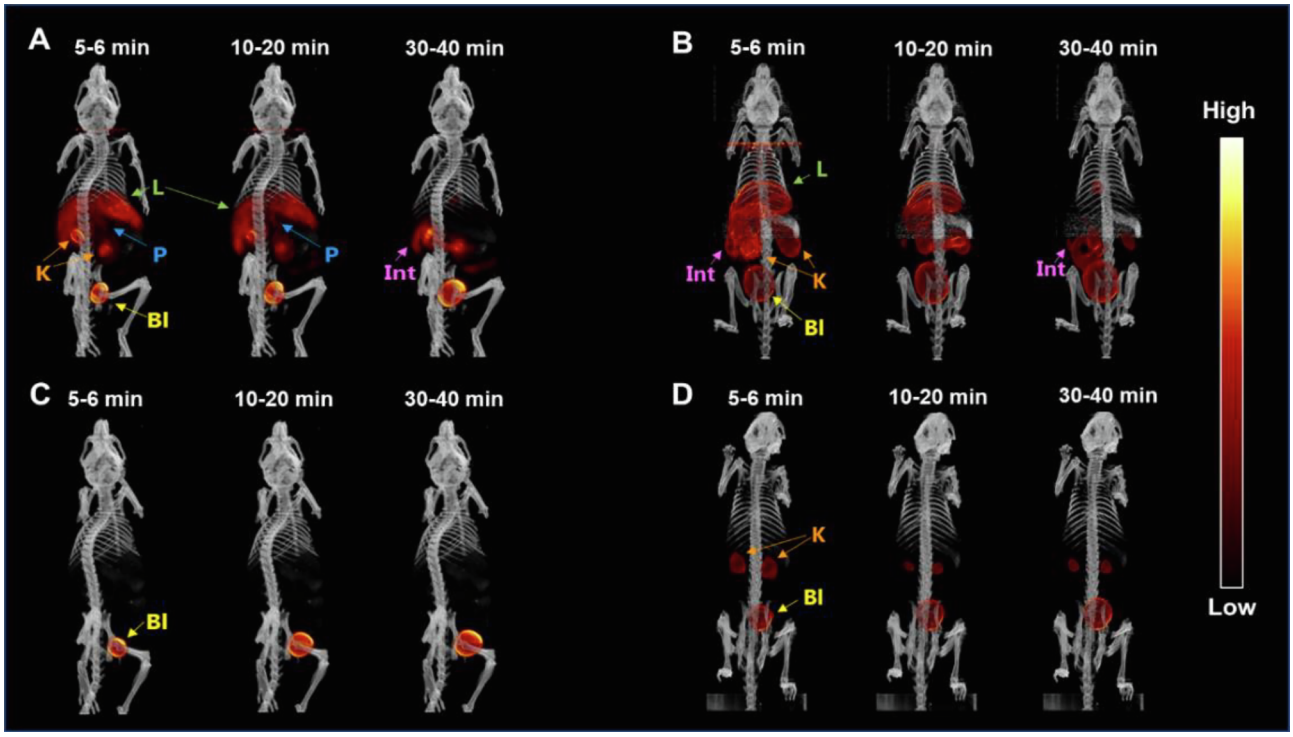

Fig. 2. PET/CT images of mice after administration of the ^{18}F-labeled STZ derivatives. (A) [^{18}F]**7a** (17.2 MBq), (B) [^{18}F]**7b** (13.4 MBq), (C) [^{18}F]**6a** (28.0 MBq), (D) [^{18}F]**6b** (33.7 MBq).

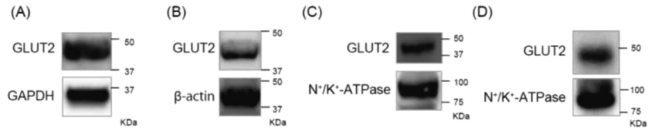

Fig. 3. The expression of GLUT2 in liver, pancreas, kidney, and small intestine. (A and B) GLUT2 expression in total protein of liver (A) and pancreas (B). GAPDH and β-actin were used as the loading control. (C and D) GLUT2 expression in membrane protein of kidney (C) and small intestine (D). Na^+/K^+-ATPase was used as the loading control.

2). Non-radioactive compounds **5a** and **5b** were obtained without any byproducts after fluorinating **4a** and **4b** with tetrabutylammonium fluoride. Hydrolysis of **5a** and **5b** and subsequent nitrosylation gave the desired products **7a** and **7b**. As expected, the ureas **6a**, **6b**, **7a**, and **7b** were relatively stable under various chromatographic purification conditions. However, **7a** and **7b** were not stable under reversed-phase high performance liquid chromatography (HPLC) conditions.

We synthesized radioactive [^{18}F]**7a** and [^{18}F]**7b** as illustrated in Scheme 4. Nucleophilic substitution of **4a** and **4b** was performed using potassium [^{18}F]fluoride. Acetonitrile was a more suitable solvent for this reaction than tetrahydrofuran and 1,4-dioxane. Ten minutes was insufficient for the reaction to go to completion, so the reaction was allowed to proceed for 20 min. The mixture was heated to 90 °C for ^{18}F-fluorination, and methanolysis was performed immediately after removing the solvent to yield [^{18}F]**6a** and [^{18}F]**6b**. [^{18}F]**6a** and [^{18}F]**6b** were purified and analyzed using a reversed-phase HPLC system equipped with a radioisotope detector. Final nitrosylation proceeded rapidly to afford [^{18}F]**7a** and [^{18}F]**7b**, which were then purified on a reversed-phase Sep-Pak solid phase extraction column. The radiochemical purities were estimated via autoradiography using thin-layer chromatography plates and found to be near 90% (84%–99%).

PET imaging was performed using normal mice to evaluate the dynamic whole-body distributions of the ^{18}F-labeled STZ derivatives. Male ddY mice were anesthetized with isoflurane and injected intravenously with [^{18}F]**7a** or [^{18}F]**7b**. [^{18}F]**6a** and [^{18}F]**6b**, which were denitroso intermediates in the synthesis of [^{18}F]**7a** and **7b**, were also examined. In an *in-vitro* study of fluorescently-labeled STZ derivatives,[35,36] it was found that denitroso derivatives were taken up by cells through GLUT2 in addition to the nitroso products. Therefore, we also expected the biodistribution of [^{18}F]**6a** and [^{18}F]**6b** as GLUT2 imaging probes. PET data were acquired for 60 min soon after injection and reconstructed into images with dynamic frames of 12 × 15 s, 7 × 60 s and 5 × 600 s. Images at representative timepoints are shown in Fig. 2. Images of mice injected with [^{18}F]**7a** and [^{18}F]**7b** showed high levels of radioactivity accumulating in the liver and kidney within 5 min of administration. We also observed intestinal accumulation after 20 min and clearance through the liver. GLUT2 is known to be expressed primarily in the liver, kidney, and intestine.[9] In addition, we performed Western blot analysis using ddY mice of same age as used for PET study, and confirmed that GLUT2 is expressed in these tissues of ddY mice (Fig. 3). The relatively high accumulations of [^{18}F]**7a** and [^{18}F]**7b** in the liver and kidney were similar to previously reported results obtained with carbon-14-labeled STZ.[33,34] Surprisingly, [^{18}F]**6a** and [^{18}F]**6b** accumulated only in the kidney and bladder soon after administration. Based on previous reports that a fluorescein-labeled denitroso STZ derivative was recognized by GLUT2 *in-vitro*,[35,36] we thought the distribution of [^{18}F]**6a** and [^{18}F]**6b** might be attributable to rapid renal excretion. However, further examination is required. We evaluated differences arising from the stereochemistry of the anomers and found that the β anomers [^{18}F]**7b** and [^{18}F]**6b** accumulated in the kidney to a greater extent than the α anomers [^{18}F]**7a** and [^{18}F]**6a**.

The *ex-vivo* biodistributions of [^{18}F]**7a** and [^{18}F]**7b** were also investigated (Table 1). Like the PET study, marked accumulation of both compounds in the liver, kidney, and intestines was observed. Meanwhile, their clearances were relatively rapid. If [^{18}F]**7a,b** are expected to add a [^{18}F]fluorohexyl group to the 7-position nitrogen atom in guanine base by a mechanism similar to STZ alkylation,[27,32] the clearance of radioactivity from these tissue may be considered too rapid. This may be attributed to the elimination of [^{18}F]fluoride ions caused by the formation of DNA cross-linking. Nitrosourea antitumor agents such as nimustine, ranimustine, and carmustine that contain 2-

Table 1
Biodistributions of [^{18}F]**7a** and [^{18}F]**7b** in normal mice.[a]

	[^{18}F]**7a**			[^{18}F]**7b**		
	10 min	30 min	60 min	10 min	30 min	60 min
Heart	3.19 ± 0.42	2.33 ± 0.42	1.38 ± 0.47	2.76 ± 0.17	1.51 ± 0.32	0.91 ± 0.26
Lung	3.56 ± 0.35	2.34 ± 0.70	1.36 ± 0.43	3.16 ± 0.30	1.94 ± 0.45	1.02 ± 0.26
Stomach	2.38 ± 1.08	2.18 ± 0.84	1.26 ± 0.35	1.39 ± 0.40	0.84 ± 0.14	0.56 ± 0.20
Liver	11.20 ± 1.21	5.46 ± 1.19	2.53 ± 0.63	9.47 ± 0.55	4.98 ± 1.34	2.58 ± 0.75
Small intestine	4.71 ± 0.49	6.41 ± 1.55	4.91 ± 1.20	6.42 ± 0.65	6.43 ± 1.37	4.11 ± 1.20
Large intestine	3.14 ± 0.19	4.79 ± 0.80	4.64 ± 1.13	2.75 ± 0.36	2.87 ± 0.40	2.32 ± 1.08
Pancreas	3.10 ± 0.14	2.28 ± 0.66	1.35 ± 0.53	3.19 ± 0.52	1.97 ± 0.56	1.16 ± 0.43
Spleen	2.47 ± 0.15	2.03 ± 0.47	1.18 ± 0.46	2.66 ± 0.37	1.47 ± 0.18	0.89 ± 0.26
Kidney	7.77 ± 1.02	10.57 ± 3.57	4.85 ± 0.80	10.31 ± 1.92	8.37 ± 1.50	4.65 ± 2.58
Bone	6.27 ± 0.98	12.94 ± 3.53	13.91 ± 5.97	1.86 ± 0.28	3.54 ± 0.92	4.08 ± 1.27
Brain	0.35 ± 0.06	0.58 ± 0.10	0.59 ± 0.15	0.24 ± 0.12	0.27 ± 0.09	0.24 ± 0.07
Blood	2.69 ± 0.24	2.09 ± 0.82	1.26 ± 0.33	2.70 ± 0.19	1.55 ± 0.24	0.91 ± 0.27

[a]Values are reported as the mean percentage of the injected dose per gram of tissue ± SD (n = 4).

chloroethyl groups are known to cause interstrand DNA cross-linking through the formation of 2-chloroethyl adducts and subsequent nucleophilic displacement of chlorine.[46] Furthermore, there are some reports which suggest that nitrosoureas with fluoroalkyl group, whose reactivity is less than that of chloroalkyl group, form DNA cross-linking.[37,46] Indeed, the accumulations of radioactivity in bone increased over time; this is associated with the presence of free fluoride ions. On the contrary, the pancreas did not show high accumulation. GLUT2 in the pancreas is present in pancreatic islet cell which is less than 5% of all pancreatic cells, so it is expected to be lower than in the liver and small intestine. Therefore, it is beneficial to evaluate the retention capability of radioactivity in pancreas for the investigation of pancreatic islet imaging probe. However, because the pancreatic accumulation is also rapidly cleared, it would be necessary to redesign a molecule that is difficult to be cleared from islet cells. Moreover, unlike [^{18}F]FDG, the compounds did not accumulate to a notable extent in the brain and heart.[8]

The chemical stability of a PET probe is important to ensure the reliability of a molecular biological evaluation. With this in mind, we synthesized STZ derivatives as glycoside analogs and radiolabeled them by introducing ^{18}F to hexyl groups at the 3′-positions. The ^{18}F-labeled STZ derivatives [^{18}F]**7a** and [^{18}F]**7b** obtained using our radiosynthetic protocol were relatively stable during purification and purity analysis. Their biodistributions clearly differed from that of [^{18}F]FDG.[47] They were similar to the biodistribution of 2-deoxy-2-[^{18}F]fluoroarabinose, a PET probe reported for the visualization of ribose salvage via GLUT2.[23] We expected that probes **6a** and **6b** would be taken up by cells after labeling the alkyl functional groups with ^{18}F, and we examined their biodistributions by performing PET imaging. However, to obtain high-contrast images, additional structural optimization is needed to suppress the dissociation of fluoride ions.

Declaration of Competing Interest

The authors declare that they have no known competing financial interests or personal relationships that could have appeared to influence the work reported in this paper.

Acknowledgments

This work was supported by Grant-in-Aid for Young Scientists (Grant Number JP18K15608) of the Japan Society for the Promotion of Science (JSPS). We thank Dr. Yasunao Hattori and Dr. Tomoshige Ando of the Center for Instrumental Analysis of Kyoto Pharmaceutical University for their technical assistance.

Appendix A. Supplementary data

Supplementary data to this article can be found online at https://doi.org/10.1016/j.bmcl.2020.127400.

References

1. Olson AL, Pessin JE. Structure, function, and regulation of the mammalian facilitative glucose transporter gene family. *Annu Rev Nutr.* 1996;16:235–256.
2. Joost HG, Thorens B. The extended GLUT-family of sugar/polyol transport facilitators: nomenclature, sequence characteristics, and potential function of its novel members (review). *Mol Membr Biol.* 2001;18:247–256.
3. Mueckler M, Thorens B. The SLC2 (GLUT) family of membrane transporters. *Mol Asp Med.* 2013;34:121–138.
4. Kasahara M, Hinkle PC. Reconstitution and purification of the D-glucose transporter from human erythrocytes. *J Biol Chem.* 1977;252:7384–7390.
5. Dick AP, Harik SI, Klip A, Walker DM. Identification and characterization of the glucose transporter of the blood-brain barrier by cytochalasin B binding and immunological reactivity. *Proc Natl Acad Sci USA.* 1984;81:7233–7237.
6. Pardridge WM, Boado RJ, Farrell CR. Brain-type glucose transporter (GLUT-1) is selectively localized to the blood-brain barrier. Studies with quantitative western blotting and in situ hybridization. *J Biol Chem.* 1990;265:18035–18040.
7. Maher F, Vannucci SJ, Simpson IA. Glucose transporter proteins in brain. *FASEB J.* 1994;8:1003–1011.
8. Phelps ME. *PET: molecular imaging and its biological applications.* New York, NY: Springer-Verlag; 2004.
9. Thorens B, Cheng ZQ, Brown D, Lodish HF. Liver glucose transporter: a basolateral protein in hepatocytes and intestine and kidney cells. *Am J Physiol.* 1990;259(6 Pt 1):C279–C285.
10. Thorens B. Molecular and cellular physiology of GLUT2, a high-Km facilitated diffusion glucose transporter. *Int Rev Cytol.* 1992;137A:209–238.
11. Johnson JH, Ogawa A, Chen L, et al. Underexpression of beta cell high Km glucose transporters in noninsulin-dependent diabetes. *Science.* 1990;250(4980):546–549.
12. Orci L, Ravazzola M, Baetens D, et al. Evidence that down-regulation of β-cell glucose transporters in noninsulin-dependent diabetes may be the cause of diabetic hyperglycemia. *Proc Natl Acad Sci USA.* 1990;87:9953–9957.
13. Unger RH. Diabetic hyperglycemia: link to impaired glucose transport in pancreatic β cells. *Science.* 1991;251(4998):1200–1205.
14. Valera A, Solanes G, Fernańdez-Alvarez J, et al. Expression of GLUT2 antisense RNA in b cells of transgenic mice leads to diabetes. *J Biol Chem.* 1994;269:28543–28546.
15. Guillam MT, Hümmler E, Schaerer E, et al. Early diabetes and abnormal postnatal pancreatic islet development in mice lacking, Glut-2. *Nat Genet.* 1997;17:327–330.
16. Guillam MT, Dupraz P, Thorens B. Glucose uptake, utilization, and signaling in GLUT2-null islets. *Diabetes.* 2000;49:1485–1491.
17. Del Guerra S, Lupi R, Marselli L, et al. Functional and molecular defects of pancreatic islets in human type 2 diabetes. *Diabetes.* 2005;54:727–735.
18. Gremlich S, Roduit R, Thorens B. Dexamethasone induces posttranslational degradation of GLUT2 and inhibition of insulin secretion in isolated pancreatic β cells. *J Biol Chem.* 1997;272:3216–3222.
19. Reimer MK, Ahren B. Altered β-cell distribution of pdx-1 and GLUT2 after a short-term challenge with a high-fat diet in C57BL/6J mice. *Diabetes.* 2002;51(1):S138–S143.
20. Ohtsubo K, Takamatsu S, Minowa MT, Yoshida A, Takeuchi M, Marth JD. Dietary and genetic control of glucose transporter 2 glycosylation promotes insulin secretion in suppressing diabetes. *Cell.* 2005;123:1307–1321.
21. Ohtsubo K, Takamatsu S, Gao C, Korekane H, Kurosawa TM, Taniguchi N. N-glycosylation modulates the membrane sub-domain distribution and activity of glucose

transporter 2 in pancreatic beta cells. *Biochem Biophys Res Commun.* 2013;434:346–351.
22. Ohtsubo K, Chen MZ, Olefsky JM, Marth JD. Pathway to diabetes through attenuation of pancreatic beta cell glycosylation and glucose transport. *Nat Med.* 2014;17(9):1067–1075.
23. Clark PM, Flores G, Evdokimov NM, et al. Positron emission tomography probe demonstrates a striking concentration of ribose salvage in the liver. *Proc Natl Acad Sci USA.* 2014;111(28):E2866–E2874.
24. Herr RR, Jahnke HK, Argoudelis AD. Structure of streptozotocin. *J Am Chem Soc.* 1967;89(18):4808–4809.
25. Schnedl WJ, Ferber S, Johnson JH, Newgard CB. STZ Transport and cytotoxicity, Specific enhancement in GLUT2-expressing cells. *Diabetes.* 1994;43:1326–1333.
26. Wang Z, Gleichmann H. GLUT2 in pancreatic islets, Crucial target molecule in diabetes induced with multiple low doses of streptozotocin in mice. *Diabetes.* 1998;47:50–56.
27. Bennett RA, Pegg AE. Alkylation of DNA in rat tissues following administration of streptozotocin. *Cancer Res.* 1981;41:2786–2790.
28. Vavra JJ, Deboer C, Dietz A, Hanka LJ, Sokolski WT. Streptozotocin, a new antibacterial antibiotic. *Antibiot Annu.* 1959;7:230–235.
29. Brentjens R, Saltz L. Islet cell tumors of the pancreas: the medical oncologist's perspective. *Surg Clin North Am.* 2001;81:527–542.
30. Wilson GL, Leiter EH. Streptozotocin interactions with pancreatic β cells and the induction of insulin-dependent diabetes. In: Dyrberg T, eds. The role of viruses and the immune system in diabetes mellitus (part of the "Current Topics in Microbiology and Immunology" book series). Berlin, Heidelberg: Springer; 1990;156:27–54.
31. Mansford KR, Opie L. Comparison of metabolic abnormalities in diabetes mellitus induced by streptozotocin or alloxan. *Lancet.* 1968;291:670–671.
32. Szkudelski T. The mechanism of alloxan and streptozotocin action in B cells of the rat pancreas. *Physiol Res.* 2001;50:536–546.
33. Karunanayake EH, Hearse DJ, Mellows G. The synthesis of [^{14}C]streptozotocin and its distribution and excretion in the rat. *Biochem J.* 1974;142:673–683.
34. Anderson T, Schein PS, McMenamin MG, Cooney DA. Correlation with extent of depression of pancreatic islet nicotinamide adenine dinucleotide. *J Clin Invest.* 1974;54:672–677.
35. Ran C, Pantazopoulos P, Medarova Z, Moore A. Synthesis and testing of beta-cell-specific streptozotocin-derived near-infrared imaging probes. *Angew Chem Int Ed.* 2007;46:8998–9001.
36. Virreira M, Popescu I, Gillet C, et al. Immunocytochemistry of GLUT2, uptake of fluorescent desnitroso-streptozotocin analogs and phosphorylation of D-glucose in INS-1E cells. *Mol Med Rep.* 2013;8:473–479.
37. Johnston TP, Kussner CL, Carter RL, et al. Studies on synthesis and anticancer activity of selected N-(2-fluoroethyl)-N-nitrosoureas. *J Med Chem.* 1984;27:1422–1426.
38. Takeda K, Akagi Y, Saiki A, Tsukahara T, Ogura H. Convenient methods for syntheses of active carbamates, ureas and nitrosoureas using N, N-disuccinimido carbonate (DSC). *Tetrahedron Lett.* 1983;24(42):4569–4572.
39. Gilissen C, Bormans G, de Groot T, Verbruggen A. Synthesis of *N*-(2-[^{18}F]fluoroethyl)-*N'*-methylthiourea: a hydrogen peroxide scavenger. *J Labelled Compd Radiopharm.* 1998;XLI:491–502.
40. Hammer CF, Loranger RA, Schein PS. Structures of the decomposition products of chlorozotocin: new intramolecular carbamates of 2-amino-2-deoxyhexoses. *J Org Chem.* 1981;46:1521–1531.
41. Avalos M, Babiano R, Cintas P, Jiménez JL, Palacios JC, Valencia C. The reaction of 2-amino-2-deoxyhexopyranoses with isocyanates. Synthesis of ureas and their transformation into heterocyclic derivatives. *Tetrahedron.* 1993;49(13):2655–2675.
42. Iwasaki M, Ueno M, Ninomiya K, Sekine J, Nagamatsu Y, Kimura G. Alkyl streptozotocin analogues with improved biological activities. *J Med Chem.* 1976;19(7):918–923.
43. Suami T, Machinami T. A synthesis of streptozotocin derivatives. *Bull Chem Soc Jpn.* 1970;43:3013–3015.
44. Bannister B. The synthesis and biological activities of some analogs of streptozotocin. *J Antibiot.* 1972;25(7):377–386.
45. Chargaff E, Bovarnich M. A method for the isolation of glucosamine. *J Biol Chem.* 1937;118:421–426.
46. Kohn KW. Interstrand cross-linking of DNA by 1,3-bis(2-chloroethyl)-1-nitrosourea and other 1-(2-haloethyl)-1-nitrosoureas. *Cancer Res.* 1977;37:1450–1454.
47. Fueger BJ, Czernin J, Hildebrandt I, et al. Impact of animal handling on the results of ^{18}F-FDG PET studies in mice. *J Nucl Med.* 2006;47(6):999–1006.